Clinical Radiology 74 (2019) 571.e9–571.e18

Contents lists available at ScienceDirect

Clinical Radiology

journal homepage: www.clinicalradiologyonline.net

Diagnostic value of 3 T MR spectroscopy, diffusion-weighted MRI, and apparent diffusion coefficient value for distinguishing benign from malignant myometrial tumours

P. Rahimifar [a], H. Hashemi [a], M. Malek [a,*], S. Ebrahimi [a], E. Tabibian [a], A. Alidoosti [a], A. Mousavi [b], F. Yarandi [b]

[a] Department of Radiology, Medical Imaging Center, Imam Khomeini Hospital Complex (IKHC), Tehran University of Medical Sciences (TUMS), Tehran, Iran
[b] Department of Gynecologic Oncology, Tehran University of Medical Sciences (TUMS), Tehran, Iran

ARTICLE INFORMATION

Article history:
Received 5 March 2018
Accepted 13 March 2019

AIM: To further verify the effectiveness of diffusion-weighted (DWI) magnetic resonance imaging (MRI) and ^{1}H magnetic resonance spectroscopy (MRS) using a 3 T MRI system to differentiate benign leiomyomas from uterine sarcoma; to investigate the benefit of adding MRS to the apparent diffusion coefficient (ADC) for improving the specificity of the benign/malignant classification.

MATERIALS AND METHODS: The dataset included 21 uterine sarcoma from 14 patients and 84 benign leiomyomas from 51 patients. T1-and T2-weighted images as well as DWI were obtained using a 3-T MRI system. Approximately 60% of patients also underwent MRS. The chi-square test was used to compare the percentage of malignant lesions that showed choline peaks, lipid peaks, and restricted diffusion to the corresponding percentage of benign masses. Using the area under a receiver operating characteristic (AUC) curve, the efficacy of different parameters for distinguishing uterine sarcomas from leiomyomas was measured.

RESULTS: The visual assessment of DWI images showed that 100% of malignant lesions exhibited restricted diffusion while the corresponding figure for benign leiomyomas was only 5%. The mean ADC of malignant tumours differed significantly from that of benign ones ($p<0.001$). The percentage of malignant lesions for which choline and lipid peaks were present was significantly higher than that of benign lesions. By combining the ADC and MRS findings, an accuracy of 98.3 (95.1–100) was achieved.

CONCLUSIONS: The findings suggested that a combination of DWI and MRS could be useful in the preoperative assessment of uterine masses to differentiate benign leiomyomas from leiomyosarcoma.

* Guarantor and correspondent: M. Malek, Department of Radiology, Medical Imaging Center, Imam Khomeini Hospital Complex (IKHC), End of Keshavarz Blvd, Tehran, 1419733141, Iran. Tel.: +98 21 61190; fax: + 98 21 6658 1615.
E-mail addresses: malek.mahrouz18@gmail.com, mmalek@tumc.ac.ir (M. Malek).

https://doi.org/10.1016/j.crad.2019.03.011
0009-9260/

Introduction

Benign leiomyomas are the most prevalent pelvic tumours among women. Fortunately, with the appropriate treatment, the prognosis is typically favourable. In contrast, uterine sarcomas are uncommon and have a poor prognosis.[1–4] Among different types of uterine sarcomas, leiomyosarcoma is the most common and shares several features with leiomyomas. Both usually present as a myometrial lesion. Although some preoperative findings can help to differentiate benign leiomyomas from uterine sarcomas, there is a significant overlap in their characteristics.[3]

Previously, benign leiomyomas were treated through hysterectomy; postoperative histopathology analysis was performed to determine the presence of uterine sarcoma and further treatment was provided to women with malignancies. Therefore, no sarcoma was missed. Today, however, benign leiomyomas are mostly treated using less invasive uterine-preserving alternatives such as gonadotropin-releasing hormone analogues[5] or uterine arterial embolisation.[6] Therefore, the accurate preoperative identification of uterine sarcoma is vital to select the appropriate treatment, particularly for patients of reproductive age.

Previous studies suggested that magnetic resonance imaging (MRI) plays a crucial role in the preoperative evaluation of uterine masses and assists in the selection of an appropriate treatment regimen for each patient.[7] Studies of the MRI appearance of uterine masses revealed that uterine sarcomas typically appear as hyper-signal lesions whereas leiomyomas are mostly characterised as well-defined hyposignal lesions on T2-weighted images.[8,9] Leiomyoma, however, can exhibit an unusual appearance, and could, therefore, be misdiagnosed as uterine sarcoma.[8,10–14] For example, haemorrhage or cystic degeneration and necrosis may be observed in leiomyomas, although in most cases the presence of necrosis is suggestive of a leiomyosarcoma.[11] As a result of this overlap between malignant and benign lesions and lack of standardised diagnostic criteria, in current practice, patients with lesions presenting mixed characteristics are treated with a hysterectomy, although some could benefit from a less-invasive uterine-preserving treatment.

Diffusion-weighted imaging (DWI) is an emerging imaging technique that typically displays malignant lesions as a hyperintense region with excellent tissue contrast.[15] Using DWI, the apparent diffusion coefficient (ADC) value, which is a quantitative measurement associated with the nuclear-to-cytoplasm ratio and cellular density of tissue, can be also obtained.[16] Previous studies indicated the usefulness of DWI and ADC for distinguishing benign conditions from malignancies in different organs, such as bowel,[17] lung,[16] breast,[15] and ovaries.[18] It has been also used for assessing female pelvic masses in a few studies. For example, in19, it was shown that DWI can be utilised for the differentiation of completely hyalinised uterine leiomyomas from ordinary leiomyomas and in20, the value of DWI and ADC in distinguishing uterine adenomyosis from leiomyoma has been investigated. In addition, a few small studies[13,14,21] showed that the DWI and ADC values could be potentially utilised for distinguishing uterine sarcomas from benign leiomyomas. Recently, Li *et al.*[22] indicated that uterine leiomyosarcoma can be differentiated from degenerated leiomyoma using DWI and ADC; however, in the present study,[22] images were acquired using 1.5-T MRI systems. Namimoto *et al.*[23] investigated the discriminative power of DWI images acquired using a 3 T unit. Although the mean ADC differed significantly between leiomyosarcoma and leiomyomas, a considerable overlap between two lesion types was observed.[23] It was also shown that a combination of T2-weighted sequences and ADC improved both sensitivity and specificity for distinguishing leiomyosarcoma from leiomyomas compared to ADC.[23]

In vivo ^{1}H magnetic resonance spectroscopy (MRS) is a non-invasive imaging technique that provides a marker of biochemical processes related to metabolic information and the transformation of normal to malignant tissue and the presence of active tumours.[24,25] MRS has been adopted for studying diseases in different body organs and the presence of various metabolite peaks. Early studies utilised MRS mainly to investigate metabolic changes in diseases affecting the brain such as Alzheimer's disease, seizure disorders, strokes, and brain tumours.[26] Later, MRS was applied for the assessing tumours in other sites such as the breast,[24,25,27–31] prostate,[32,33] bowel,[34] ovaries,[35] and uterus[36,37]; however, findings related to the efficacy of MRS are still controversial. For example, in the case of breast cancer, several previous studies[24,25,27–31] have indicated that MRS could potentially be used to distinguish breast malignancies from benign conditions, and the presence of choline peak in MRS spectra was associated with malignancies. Other findings, however, suggested that choline peaks might also be present in some benign conditions such as fibroadenomas or tubular adenomas.[25,38]

A preliminary study on Japanese women revealed that the presence of a choline peak in MRS spectra obtained using 3-T scanner could be used to differentiate benign uterine masses from the malignant ones.[36] The study achieved a sensitivity of 93% and a specificity of 83% for the benign/malignant categorisation.[36] In another study, Takeuchi *et al.*[37] focused on the presence of a high lipid peak on MRS spectra and showed that it is an indicator of uterine sarcoma and hence MRS could be beneficial in differentiating uterine sarcomas. They included 26 leiomyomas and 12 uterine sarcomas and obtained a sensitivity of 100% and specificity of 96%.[37] In another study, Zhang *et al.*[39] investigated whether the presence of the choline peak was suggestive of a malignant lesion and demonstrated that the MRS was able to distinguish endometrial cancer from benign lesions.

The aim of the present study was to (i) further validate the effectiveness of DWI and the ADC value using a 3-T scanner to differentiate benign leiomyomas from leiomyosarcomas on a larger number of lesions; (ii) further verify the feasibility of adopting MRS (the presence of choline and

lipid peaks) to distinguish benign leiomyomas from leiomyosarcomas on a larger cohort; and (iii) investigate the benefit of adding MRS to ADC for improving the specificity of malignancy detection. To the authors' knowledge, no previous study has investigated the added benefit of MRS to DWI in the differentiation of uterine masses from leiomyomas. In addition to further verification of the efficacy of DWI and MRS in distinguishing benign lesions from malignancies, this study sought to explore whether MRS provides complementary information to the ADC to improve the specificity of the malignant/benign categorisation.

Materials and methods

Patients

The study was approved by the institutional ethical review board. Signed informed consent forms were obtained from all patients who participated in the study. All women with suspicious myometrial masses referred to the department for 3 T MRI assessment preoperatively from September 2014 to September 2015 were included. Patients who weighed >100 kg or had an electronic implant, such as an inner ear prosthesis, pacemaker, neuron stimulator, or insulin pump, were excluded. The ultimate diagnosis of each lesion was made on a pathological specimen obtained after hysterectomy, based on the consensus opinion of experienced pathologists. Only patients who underwent hysterectomies and those with benign or malignant myometrial tumours were included.

Sixty-five women confirmed to have a total of 105 masses were included. Patient age, menopausal status, and lesion size were recorded. Fourteen women (21.5% of patients) included in the study had a diagnosis of malignancy (the specimen contained at least one malignant mass). Overall, of 105 lesions, 21 were malignant whereas the remainder were benign. The average age of patients in the benign and malignant groups was 42.8±13.3 and 39.5±11.2, respectively. Approximately 62% of lesions belonged to premenopausal women in both groups. Table 1 summarises the patients' characteristics in each group.

Imaging protocol

All included patients were examined using a 3 T MRI system (Magnetom Trio, Siemens, Erlangen, Germany). The patients were asked to fast for 3 hours before the imaging. Immediately before commencement of the scan, 20 mg hyoscine butylbromide was administered intravenously. Previous studies have recommended administration of an intra-muscular anti-peristaltic agent such as hyoscine butylbromide in oncological MRI as it improves lesion visualisation.[40] The routine pelvic MRI protocol was performed prior to the acquisition of DWI images. DWI images were acquired using a single-shot echo-planar sequence in the axial plane with a section thickness of 4 mm, an intersection gap of 0.8 mm, and field-of-view of 280 mm. For four benign lesions, DWI was noisy and inconclusive, so they were excluded from the study. All patients were positioned supine on the scanner table with their pelvis centred on the phased-array coil.

Patients also underwent MRS using a point-resolved spectroscopy sequence (PRESS) technique, and single-voxel water-suppressed spectroscopy with automatic shimming was performed in patients. By referring T1-and T2-weighted images as well as DWI sequences, an experienced technologist under the guidance of a radiologist placed a single $2\times2\times2cm^3$ cubic spectroscopic volume-of-interest over the mass areas so that cystic or necrotic areas, large vessels, calcification, and haemorrhage were excluded where possible. The total data acquisition time was approximately 5 minutes. Approximately 60% of MRS data were approved by a physicist according to background noise.

Image analysis

The magnitude of diffusion sensitisation in DWI is defined by the b value. From the DWI images, the ADC maps were automatically generated on a pixel-by-pixel basis using (1) where b_0 and b_1 represent lower and higher b values, respectively, while S_0 and S_1 are the corresponding signal intensity for these b values. The calculations were done offline using an in-house software and b_1 and b_0 were set to 0 and 1000 sec/mm^2, respectively.

$$\text{Diffusion coefficiency} = \frac{-(\ln(S_1) - \ln(S_2))}{(b_1 - b_0)} \quad (1)$$

To calculate the ADC value of the mass, an experienced radiologist determined the region of Interest (ROI), which encompassed the solid part of the tumour, while avoiding healthy tissues and myometrium, and the ADC mean value was calculated over the ROI.[41]

Previous studies indicated that malignant lesions typically exhibit considerably high signal intensity on high b value images, as a result of water diffusion restriction in the dense cellular area with larger cells.[42,43] Therefore, the signal intensity of DWI images (presence of diffusion restriction) for a b value of 1,000 s/mm^2 and ADC signal were also visually assessed within the solid area of the tumour by an experienced radiologist. When the lesion had a high signal on b=1,000 s/mm^2 and low on ADC map, it classified in the restricted group.

Table 1
Patients' characteristics.

	No. of patients (%)	No. of lesions (%)	Premenopausal women (%)	Age (mean±SD, range), year	Lesion size (mean±SD, range), mm
Benign	51 (78.5%)	84 (80%)	52 (61.9%)	42.8±13.3 (21–66)	68.2±41.8 (8–219)
Malignant	14 (21.5%)	21 (20%)	13 (61.9%)	39.5±11.2 (18–68)	79.5±79.5 (20–192)
Overall	65	105	65 (61.9%)	42.1±11.7 (18–68)	70.5±45.1 (8–219)

The raw acquired spectroscopy data were processed off-line with an in-house computer software involved a Fourier transformation, automatic frequency shift correction, and baseline correction, followed by an automatic voxel-specific phase correction based on choline and lipid peaks, and automatic voxel-specific curve fitting. The detection of apparent resonance peaks at 1.33 and 3.23 ppm were corresponding to the lipid and choline respectively. The lipid and choline concentration levels were evaluated visually and images were categorised into two classes, i.e. positive and negative, compared to the noise level by visual estimation.

Statistical analysis

The statistical tests have been used to assure the baseline characteristics were matched between benign and malignant lesions. The lesion size and patients' age were compared between two lesion types utilising two independent sample *t*-test. Moreover, the chi-square test was used to compare the percentage of premenopausal women between the two groups.

The percentages of lesions that showed restricted diffusion were compared between the benign and malignant groups using the chi-square test. Similarly, the percentage of malignant lesions that exhibited a lipid peak was compared with that of benign lesions. In addition, a chi-square test was utilised to investigate whether the percentage of lesions that manifested a choline peak differed significantly between the benign and malignant groups. All statistical analyses were performed using SPSS, version 22.0 (IBM, Armonk, NY, USA).

Using the two sample independent *t*-test, the mean ADCs of the malignant lesions were compared to those of the benign lesions. For assessing the effectiveness of ADC in differentiating benign from malignant masses, receiver operating characteristic (ROC) curves were generated and the corresponding area under ROC curve (AUC) values were calculated. An AUC value of 1 demonstrates a perfect classifier whereas a value of 0.5 shows a random classifier. The confidence intervals for AUC were computed using the bootstrap method. The knee point of the ROC curve was also extracted, which is known as the optimal operating point of the classifier where a transition from the rapid increase of sensitivity to the rapid decline of specificity occurs. A binary classifier was generated based on the ADC metric, by using the ADC value corresponding to the knee point as a cut-off threshold for categorisation of the masses either as benign or malignant.

Five measures of accuracy including sensitivity, specificity, negative predictive value (NPV), positive predictive value (PPV), and overall accuracy were extracted for the classifier based on ADC values. The classification of masses was also based on other variables, i.e., DWI restriction as well as lipid and choline MRS signals and the accuracy measures were compared to that of ADC. Finally, to investigate the added benefits of DWI and MRS, the accuracy of the classifiers was compared to that of classifiers that categorised masses based on the signal intensity of T1 and T2-weighted images. The signal intensity was assessed visually by an experienced radiologist. For all accuracy measures, 95% confidence intervals were also calculated.

Whether combining the ADC with the MRS results increased the accuracy was also investigated. To do so, a classifier was designed that categorised a lesion as a malignant one when the ADC was less than the cut-off point, and the specimen exhibited a lipid or choline peak (at least one of the peak was present). The rest of the lesions were classified as leiomyomas. The five accuracy measures were also calculated for this classifier.

Results

The two independent sample *t*-test has shown that the mean age of patients in the malignant and benign groups did not differ significantly ($p=0.25$). In addition, there was no significant difference between the malignant and benign groups regarding mean lesion size ($p=0.70$) and menopausal status ($p=1.0$). Therefore, the baseline characteristics of two groups were matched.

Table 2 presents the number and percentage of benign and malignant lesions that exhibited restricted diffusion at DWI, and choline and lipid peaks at MRS. As shown in Table 2, the percentages of positive cases for the variables differed significantly between benign and malignant groups ($p<0.001$). Fig 1 shows T2-weighted and DWI images as well as ADC map for a 45-year-old patient with multiple benign tumours. The absence of the restricted diffusion can be seen in Fig 1b and c. Fig 2 indicates similar images for a 56-year-old patient with invasive leiomyosarcoma. For this patient, MRS further validated the malignant nature of the mass as a high lipid peak was present in MRS spectra (Fig 2d).

Both Figs 1 and 2 depict typical benign and malignant tumours. Fig 3 indicates a degenerated myometrial mass. As shown in Fig 3a, the mass was seen as a hyper signal lesion on T2-weighted imaging. T2 hyperintensity is generally seen in malignant tumours, but is not specific as this feature can also be demonstrated in degenerated leiomyomas.[22] For the patient depicted in Fig 3, the DWI image, ADC map, and MRS did not support the presence of malignancy as the

Table 2
The mean, standard deviation, 95% confidence interval, and the range of the extracted quantitative variables for the entire population along with the mean values of each parameter for benign and malignant lesions.

Variable	No. missing[a]	*p*-Value	Status[b]	Positive	Negative
DWI restriction	4	<0.001	B	4 (5%)	76 (95%)
			M	21 (100%)	0 (0%)
MRS choline peak	43	<0.001	B	4 (8.2%)	45 (91.8%)
			M	9 (69.2%)	4 (30.8%)
MRS lipid peak	43	<0.001	B	2 (4%)	48 (96%)
			M	8 (61.5%)	5 (38.5%)

DWI, diffusion-weighted imaging; MRS, magnetic resonance spectroscopy.
[a] Number of cases for which the imaging was not performed.
[b] B and M represent benign and malignant groups respectively.

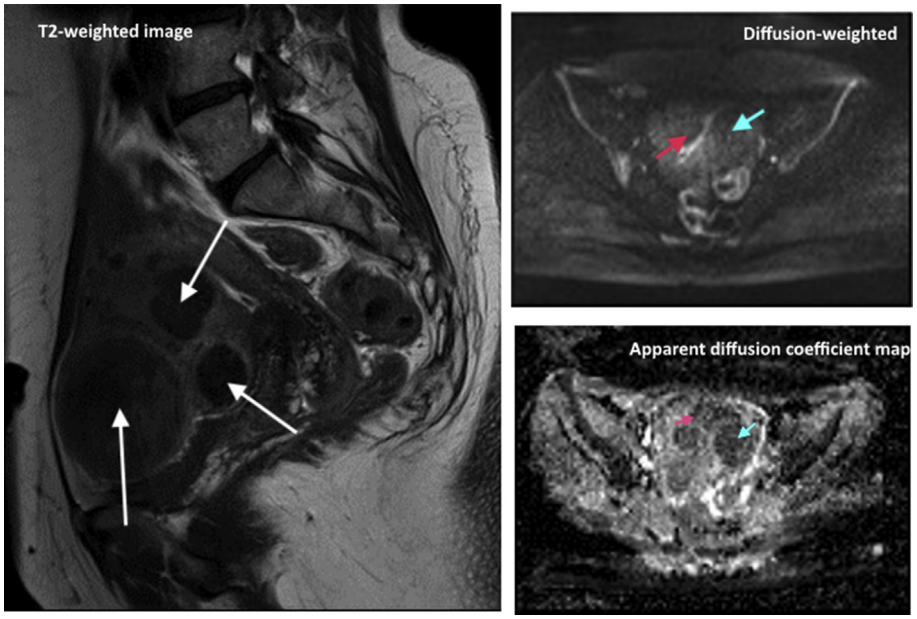

Figure 1 A 45-year-old patient with a history of abnormal uterine bleeding (AUB). Multiple typical myometrial masses were observed on the T2-weighted image (left image). Masses (white arrows) had well-defined and regular margins and showed hyposignal intensity on the T2-weighted image. DWI image (top, right image) and ADC map (bottom, right image) are also shown. According to the DWI and ADC map, the region did not demonstrate abnormal diffusion restriction. The ADC value was 1.162×10^{-3} mm^2/s. All findings were suggestive of the benign nature of the masses.

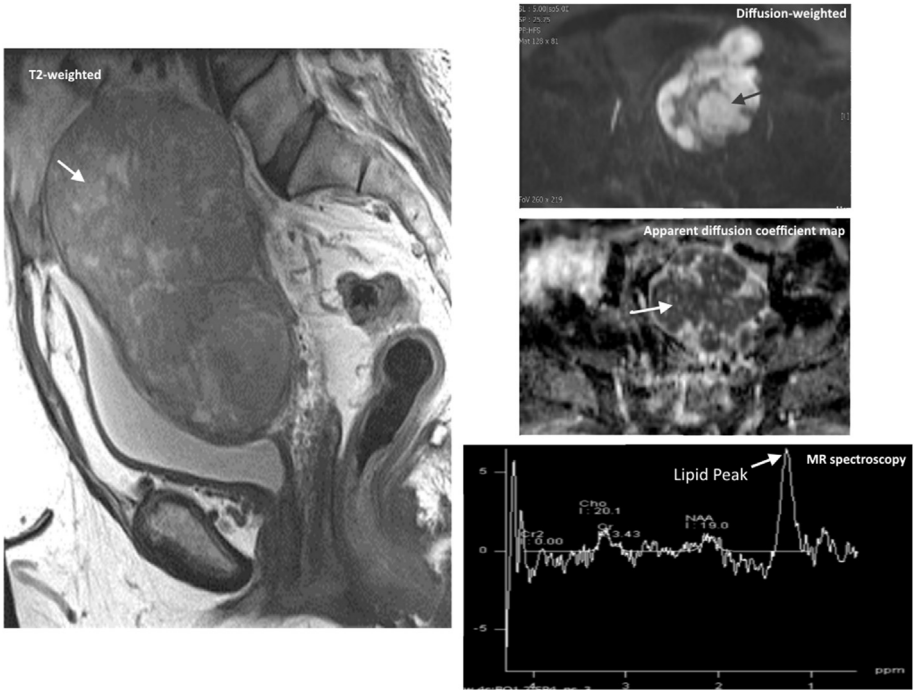

Figure 2 A 56-year-old patient with pelvic pain 6 years after total abdominal hysterectomy with bilateral salpingo-oophorectomy. A heterogeneous malignant mass (leiomyosarcoma) was observed on the T2-weighted image (left image). The heterogeneity of a mass could represent sarcoma or atypical myoma. The DWI image (top, right image) and ADC map (middle, right image) are also shown. The ADC value was 0.845×10^{-3} mm^2/s. DWI and ADC map demonstrated restricted diffusion (an indicator of uterine sarcoma). The MRS image (bottom, right image) of the mass showed a high lipid peak (an indicator of uterine sarcoma). Masses are shown using arrows.

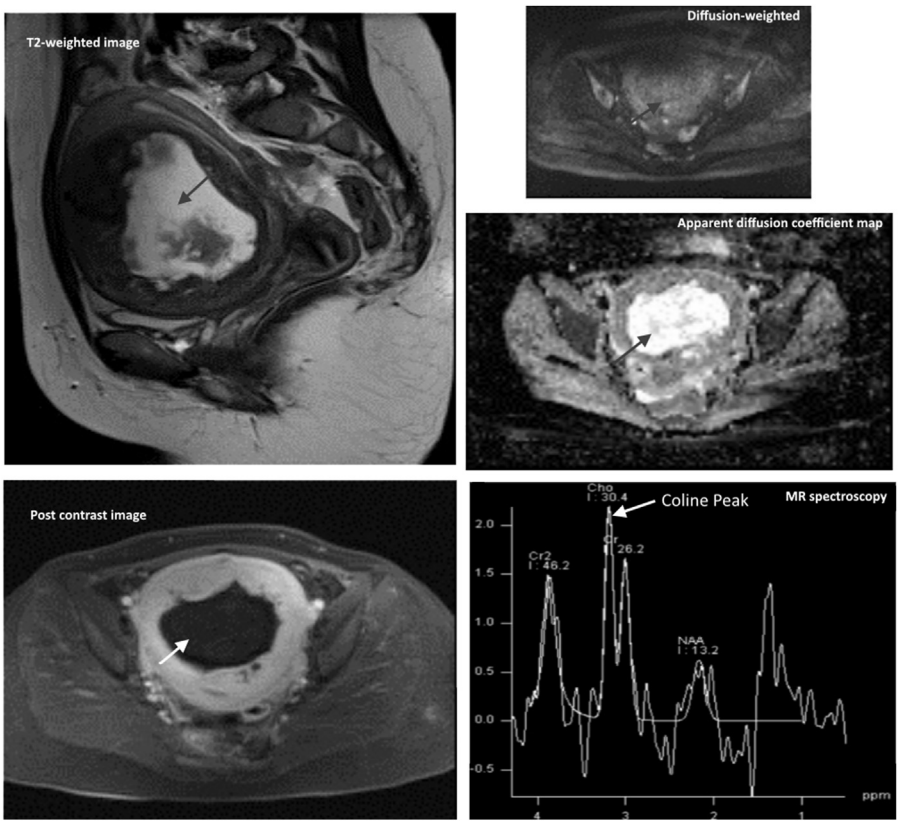

Figure 3 A 56-year-old patient with a history of abnormal uterine bleeding (AUB) and a single atypical (degenerated) myoma. The mass exhibited central high signal area on the T2-weighted image (top, left image) and central non-enhancing area on the post-contrast image (bottom, left image); findings are common features of atypical myometrial mass and uterine sarcomas. The DWI image (top, right image) and ADC map (middle, right image) are also shown. According to the DWI and ADC map, the region did not demonstrate abnormal diffusion restriction. The ADC value was 1.2×10^{-3} mm^2/s. MRS (bottom, right image) of the mass did not show a prominent choline or lipid peak. Masses are shown using arrows.

region did not demonstrate abnormal diffusion restriction and elevated choline and lipid peaks were not present in the MRS spectra.

In Fig 2d, a dominant lipid peak was indicative of the malignant nature of the tumour. The presence of a choline peak denoting increased membrane formation in a hypercellular tumour is another indicator for malignancy. In Fig 4, a histologically proven endometrial stromal sarcoma was shown. Similar to the case presented in Fig 2, T2-weighted image, DWI image, and ADC map are shown. As shown in Figs 2d and 4d, the lesion presented in Fig 2 exhibited a dominant lipid peak while a dominant choline peak was present in the one shown in Fig 4.

The distribution of the ADC values for both malignant and benign groups is indicated in Fig 5. The mean ADC of malignant tumours differed significantly from that of benign ones (0.877 ± 0.384 versus 1.426 ± 0.233, $p<0.001$). The ADC values of malignant lesions ranged from 0.573 to 1.672 while the minimum and maximum values of ADC for benign lesions were 0.000 and 2.377 respectively.

To evaluate the diagnostic value of the ADC, the ROC curve (Fig 6) was generated. The metric achieved an AUC of 92.42 (82.67–97.15), which differed significantly from chance ($p<0.001$). An optimal cut-off value (optimal decision threshold) of 1.057 was used for classifying lesions as malignant or benign. The accuracy measures for the classifier are shown in Table 3. In addition, Table 3 indicates the accuracy measures for the benign/malignant categorisation of masses based on the presence of restricted diffusion and choline and lipid peaks at MRS. The performance measures of classifiers based on signal intensity on T1-and T2-weighted images are also listed in Table 3 for comparison. As shown, both the signal intensity of T2 and DWI restriction obtained a sensitivity of 100%. Meanwhile, DWI restriction also achieved the second highest specificity, NPV, and overall accuracy among the included variables. The signal intensity of T1 resulted in the highest specificity; however, due to its low sensitivity and PPV, its diagnostic value is limited. In the last row of Table 3, the accuracy measures of the classifier, which combined the ADC with MRS findings, are indicated. The classifier categorised a lesion as a malignancy only when the ADC was less than the cut-off point, and the lesion manifested a lipid or choline peak (the presence of at least one of them). Otherwise, the masses were categorised as benign lesions. As shown, by combining the ADC with MRS findings, the highest specificity, NPV, and overall accuracy were obtained.

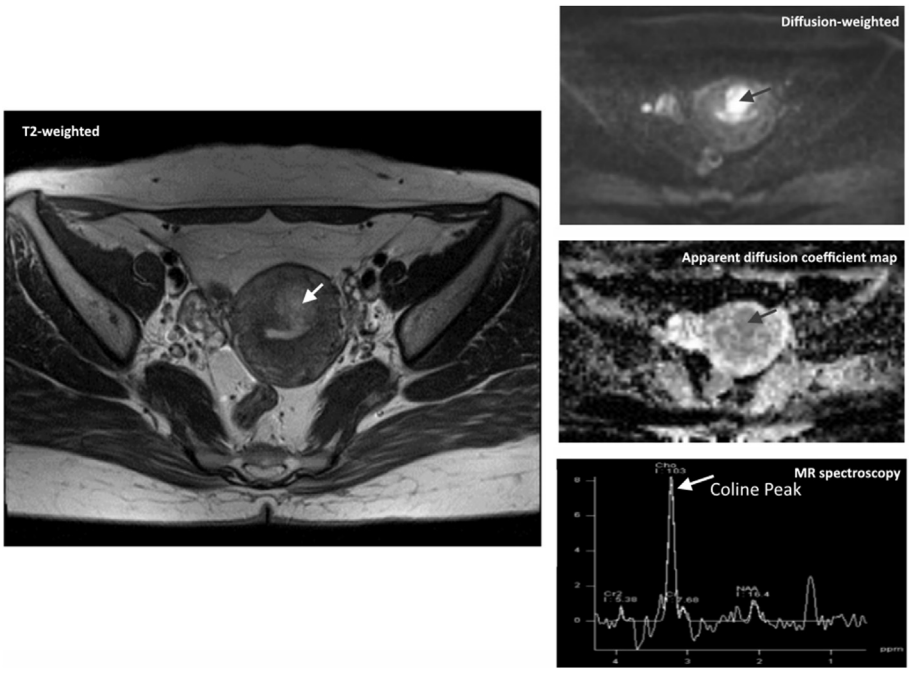

Figure 4 A 26-year-old patient with a history of abnormal uterine bleeding (AUB) and histologically proven endometrial stromal sarcoma. A heterogeneous malignant mass (leiomyosarcoma) was observed on the T2-weighted image (left image). The heterogeneity of a mass could characterise both leiomyosarcomas and atypical myometrial masses. The DWI image (top, right image) and ADC map (middle, right image) are also shown. The ADC value was 0.92×10^{-3} mm^2/s. DWI and ADC map demonstrated restricted diffusion (an indicator of uterine sarcoma). The MRS image (bottom, right image) of the mass showed a high choline peak (an indicator of uterine sarcoma). Masses are shown using arrows.

Discussion

In the present study, the usefulness of DWI for differentiating benign leiomyomas from leiomyosarcoma was studied. DWI can provide a quantitative metric of ADC, which is a marker of cellular density. The present data suggested that the ADC value has a promising discriminative power in differentiating malignant masses from benign ones. The present findings also showed that the presence of choline and lipid peaks was suggestive of leiomyosarcoma. Finally, the present results suggested that a combination of MRS and ADC could be utilised to improve the specificity of the benign/malignant classification.

Previously, it was shown that DWI and ADC can be utilised for distinguishing benign conditions from the malignancies in different organs such as breast[15] and ovaries.[18] It

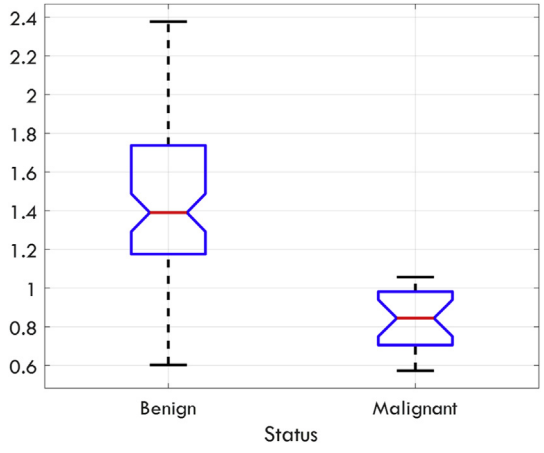

Figure 5 The distribution of ADC values across benign and malignant lesions. The red line and the notches show the median value and the 95% confidence interval for the median value. The bottom and top edges of the box indicate the first and third quartile while the whiskers extend to 1.5× the interquartile range.

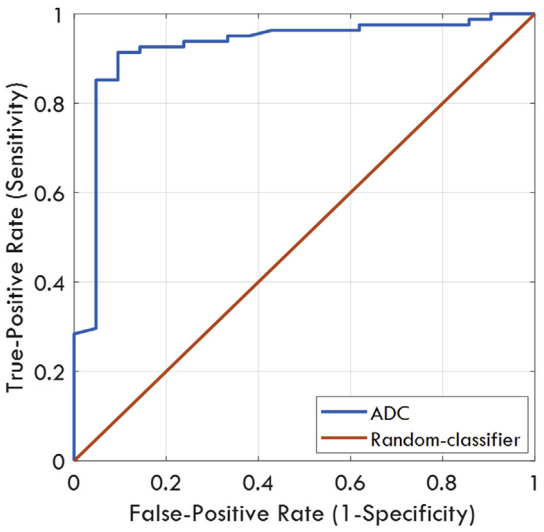

Figure 6 The ROC curve for ADC values.

Table 3
Performances of different variables in distinguishing malignant lesions from benign ones.

Variable (Cut-off Point)	Sensitivity (%)	Specificity (%)	NPV (%)	PPV (%)	Accuracy (%)
Signal intensity of T2	100 (95.6–100)	60.4 (78.6–45.7)	45.7 (36–55.6)	100 (95.6–100)	76.2 (69.3–83.0)
Signal intensity of T1	14.3 (8.5–22.6)	88.7 (98.6–42.9)	42.9 (33.4–52.9)	81.6 (72.6–88.4)	79.0 (72.5–85.6)
DWI restriction	100 (95.4–100)	88.2 (98.5–84)	84.0 (75.1–90.4)	100 (95.4–100)	96.0 (92.8–99.2)
MRS lipid	61.5 (48.4–73.3)	86.9 (99.8–80)	80.0 (67.7–88.9)	90.6 (79.9–96.6)	88.9 (82.4–95.4)
MRS choline	69.2 (56.1–80.1)	81.3 (97.5–69.2)	69.2 (56.1–80.1)	91.8 (81.3–97.5)	87.1 (80.1–94.1)
ADC	95.2 (88.5–98.6)	76.2 (91.2–62.5)	62.5 (52.3–71.8)	98.6 (93.1–100)	87.2 (81.6–92.6)
Combined[a]	90.9 (79.9–97.0)	100 (92.5–100)	100 (92.5–100)	98.0 (89.4–100)	98.3 (95.1–100)

The sensitivity, specificity, negative predictive value (NPV), positive predictive value (PPV), and accuracy are shown. The 95% confidence intervals for each measure are shown in the parentheses. The highest value in each column is shown in bold.
[a] A combination of ADC (whether the value is less than 1.06) and the MRS findings (the presence of a lipid or choline peak).

has also been utilised for distinguishing uterine sarcoma from benign leiomyomas.[13,14,21–23] The findings from the present study also suggested the usefulness of DWI and ADC for the leiomyosarcoma/benign leiomyomas classification. Table 4 indicates how the results compared with the previous similar studies aimed at utilising DWI and ADC for distinguishing benign leiomyomas from uterine sarcoma. As shown, overall the present findings are coherent with the existing literature and confirm the diagnostic value of DWI and ADC for distinguishing uterine sarcoma from benign leiomyomas. As it is indicated in Table 4, the main strength of the present study was including the larger number of malignant lesions. Moreover, the age of women in benign and malignant groups matched in the dataset, this makes the included samples more challenging regarding making the preoperative diagnosis. In addition, the present study differed from most of the previous studies regarding the MRI system used as only one of the previous studies utilised a 3 T unit for imaging.[24]In the present study, all diagnoses were confirmed with the pathologic analysis after hysterectomy; however, in24, only 35 benign cases underwent hysterectomy, and hence the diagnosis confirmed the histopathological analysis.

The present study showed that the presence of lipid and choline peaks in MRS spectra was suggestive of the leiomyosarcoma. This finding is in line with previous studies on uterine masses[36,37] and confirms the efficacy of utilising MRS for distinguishing benign from malignant uterine masses; however, the sensitivity and specificity that were achieved in the present study for benign/malignant classification were lower than that of two previous studies.[36,37] The difference could be due to variations in the nature of the masses included in the study; they included both endometrial and myometrial lesions whereas the present study was limited to myometrial lesions.

In two previous studies,[13,23] the diagnostic benefit of combining T2-weighted and DWI images were investigated. Thomassin-Naggara *et al.*[13] achieved an overall accuracy of 92.4% by combining T2-weighted, b=1000, and ADC features. In addition, Namimoto *et al.*[23] indicated that a combination of ADC and T2-weighted sequences obtained an accuracy of 100%. In the present study, the

Table 4
Comparison of the study's findings regarding DWI and ADC analysis with that of similar studies.

Study	Masses included in the study[a]	Difference between mean age[b]	Unit	Main results
[14]	10 leiomyosarcoma from 5 patients and 83 leiomyoma nodules from 76 patients	$p<0.01$	1.5 T	Sensitivity of 100%; specificity of 94%; PPV of 66.7%; NPV of 100%; overall accuracy of 94.6%
[13]	26 benign leiomyoma and 19 malignant uterine mesenchymal tumour (3 leiomyosarcomas)	$p<0.0001$	1.5 T	High b_{1000} signal intensity and mean ADC were suggestive of malignancy
[23]	8 uterine sarcomas (4 leiomyosarcomas) and 95 benign leiomyomas	Not stated	3 T	The mean ADC value differed significantly from that of leiomyomas; however, there was a considerable overlap
[22]	16 leiomyosarcoma and 26 degenerated leiomyoma	$p<0.001$	1.5 T	The mean ADC value differed significantly from that of leiomyomas. The sensitivity, specificity, accuracy, PPV, and NPV were 100%, 90%, 93%, and 83% and 100% based onb_0 and 100%, 93%, 96%, and 90% and 100% based on b=1000
[21]	7 uterine sarcomas (5 leiomyosarcomas) and 51 benign leiomyomas.	Not stated	1.5 T	The mean ADC value differed significantly from that of leiomyomas; however, there was an overlap
This study	21 leiomyosarcoma from 14 patients and 81 leiomyomas from 47 patients	$p=0.25$	3 T	The sensitivity, specificity, accuracy, PPV, and NPV based on ADC and the visual assessment of the presence of restricted diffusion were 95.2%, 76.2%, 62.5%, and 98.6% and 100%, 88.2%, 84%, and 100%.

[a] Number of leiomyosarcomas is shown in parenthesis where provided separately.
[b] If the mean age of the two groups differed significantly.

added benefit of MRS to ADC in distinguishing benign leiomyomas from uterine sarcoma was investigated with the proposed framework shown in Fig 7. The present results showed that, at the expense of <5% drop in the sensitivity, the specificity increased by approximately 24%. This finding was consistent with the studies on utilising MRS for breast cancer, where it was shown that MRS could be beneficial for improving the specificity of malignancy detection.[38]

The present study has a number of limitations. Firstly, the present cohort might not representative of all benign leiomyomas as only those patients who underwent hysterectomies were included. As the post-hysterectomy histopathological examination is the reference standard for benign/malignant differentiation, this limitation was inevitable. Secondly, although the dataset was larger than that of many previous studies, further verification of the proposed framework on a larger dataset with more borderline cases is required and conducting large-scale prospective cohort studies could be a future step. Thirdly, in the present study, a binary variable was used for describing the status of lipid and choline peaks and information about the magnitude of the peak was not used. Further investigations on the magnitude of peaks could be a potential avenue for the future work. In addition, the presence of restricted diffusion was visually assessed by an expert radiologist, and hence, was subject to inter- and intra-reader variability. In the future, these variations should be studied.

In summary, the present study provided further verification for the feasibility of using DWI and ADC in the preoperative differentiation of benign from malignant myometrial tumours. The study also showed that the presence of lipid or choline peaks was suggestive of leiomyosarcoma. Finally, the efficacy of combining the ADC with MRS results for differentiating benign myometrial lesions from malignant ones is also supported. Therefore, the proposed framework has major implications for improving the current management of uterine masses through the non-invasive detection of benign cases that could be treated less aggressively.

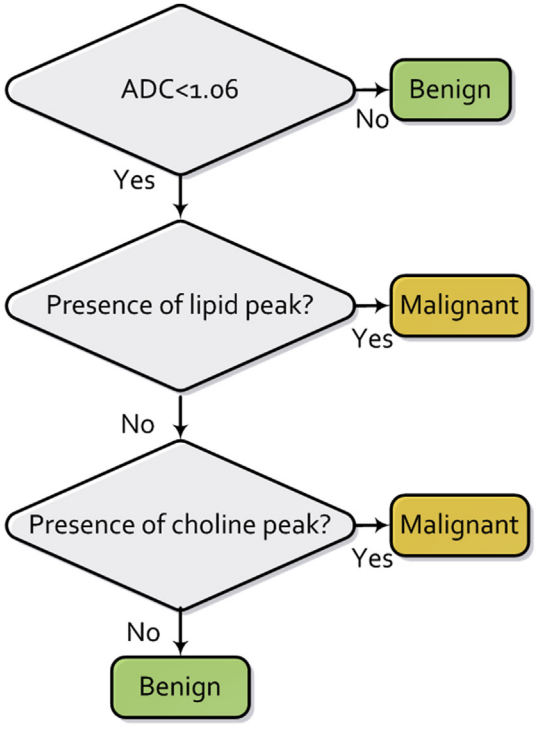

Figure 7 The flowchart of the proposed framework for distinguishing benign from malignant myometrial tumours by combining the ADC value extracted based on DWI with MRS findings.

Conflict of interest

The authors declare no conflict of interest.

Acknowledgements

The authors thank the physicians, technologists, and all other staff of the Department of Radiology, Imam Khomeini Hospital, where the data were collected. The authors are also truly grateful to all of the patients who participated in the study.

References

1. D'Angelo E, Prat J. Uterine sarcomas: a review. *Gynecol Oncol* 2010;**116**(1):131–9.
2. Khan AT, Shehmar M, Gupta JK. Uterine fibroids: current perspectives. *Int J Womens Health* 2014;**6**:95.
3. Santos P, Cunha TM. Uterine sarcomas: clinical presentation and MRI features. *Diagn Interv Radiol* 2014;**21**(1):4–9.
4. Zimmermann A, Bernuit D, Gerlinger C, *et al*. Prevalence, symptoms and management of uterine fibroids: an international internet-based survey of 21,746 women. *BMC Womens Health* 2012 Dec;**12**(1):6.
5. Colgan TJ, Pendergast S, LeBlanc M. The histopathology of uterine leiomyomas following treatment with gonadotropin-releasing hormone analogues. *Hum Pathol* 1993;**24**(10):1073–7.
6. Smith SJ. Uterine fibroid embolization. *Am Fam Physician* 2000 Jun;**61**(12):3601–14.
7. Aracki-Trenkic A, Stojanov D, Petric A, *et al*. The role of magnetic resonance imaging in the evaluation of endometrial carcinoma. *J Buon* 2016;**13**:14.
8. Sahdev A, Sohaib SA, Jacobs I, *et al*. MRI of uterine sarcomas. *AJR Am J Roentgenol* 2001 Dec;**177**(6):1307–11.
9. Hricak H, Finck S, Honda G, *et al*. MRI in the evaluation of benign uterine masses: value of gadopentetate dimeglumine-enhanced T1-weighted images. *AJR Am J Roentgenol* 1992;**158**(5):1043–50.
10. Murase E, Siegelman ES, Outwater EK, *et al*. Uterine leiomyomas: histopathologic features, MRI findings, differential diagnosis, and treatment. *RadioGraphics* 1999;**19**(5):1179–97.
11. Ueda H, Togashi K, Konishi I, *et al*. Unusual appearances of uterine leiomyomas: MRI findings and their histopathologic backgrounds. *RadioGraphics* 1999;**19**(Suppl. 1):S131–45.
12. Schwartz LB, Zawin M, Carcangiu ML, *et al*. Does pelvic magnetic resonance imaging differentiate among the histologic subtypes of uterine leiomyomata? *Fertil Steril* 1998;**70**(3):580–7.
13. Thomassin-Naggara I, Dechoux S, Bonneau C, *et al*. How to differentiate benign from malignant myometrial tumours using MRI. *Eur Radiol* 2013;**23**(8):2306–14.
14. Sato K, Yuasa N, Fujita M, *et al*. Clinical application of diffusion-weighted imaging for preoperative differentiation between uterine leiomyoma and leiomyosarcoma. *Am J Obstet Gynecol* 2014;**210**(4). 368. e1-. e8.
15. Marini C, Iacconi C, Giannelli M, *et al*. Quantitative diffusion-weighted MRI in the differential diagnosis of breast lesion. *Eur Rad* 2007;**17**(10):2646–55.

16. Matoba M, Tonami H, Kondou T, *et al*. Lung carcinoma: diffusion-weighted MRI—preliminary evaluation with apparent diffusion coefficient. *Radiology* 2007;**243**(2):570–7.
17. Nasu K, Kuroki Y, Kuroki S, *et al*. Diffusion-weighted single shot echo planar imaging of colorectal cancer using a sensitivity-encoding technique. *Jap J Clin Onc* 2004;**34**(10):620–6.
18. Takeuchi M, Matsuzaki K, Nishitani H. Diffusion-weighted magnetic resonance imaging of ovarian tumours: differentiation of benign and malignant solid components of ovarian masses. *J Comput Assist Tomogr* 2010;**34**(2):173–6.
19. Shimada K, Ohashi I, Kasahara I, *et al*. Differentiation between completely hyalinized uterine leiomyomas and ordinary leiomyomas: three-phase dynamic magnetic resonance imaging (MRI) vs. diffusion-weighted MRI with very small b-factors. *J Magn Reson Imaging* 2004;**20**(1):97–104.
20. Yang Q, Zhang LH, Su J, *et al*. The utility of diffusion-weighted MRI in differentiation of uterine adenomyosis and leiomyoma. *Eur J Radiol* 2011;**79**(2):e47–51.
21. Tamai K, Koyama T, Saga T, *et al*. The utility of diffusion-weighted MRI for differentiating uterine sarcomas from benign leiomyomas. *Eur Radiol* 2008;**18**(4):723–30.
22. Li HM, Liu J, Qiang JW, *et al*. Diffusion-weighted imaging for differentiating uterine leiomyosarcoma from degenerated leiomyoma. *J Comput Assist Tomogr* 2017;**41**(4):599–606.
23. Namimoto T, Yamashita Y, Awai K, *et al*. Combined use of T2-weighted and diffusion-weighted 3-T MRI for differentiating uterine sarcomas from benign leiomyomas. *Eur Radiol* 2009;**19**(11):2756.
24. Jagannathan NR, Sharma U. Breast tissue metabolism by magnetic resonance spectroscopy. *J Metabonomics Metab* 2017;**7**(2):25.
25. Faghihi R, Zeinali-Rafsanjani B, Mosleh-Shirazi MA, *et al*. Magnetic resonance spectroscopy and its clinical applications: a review. *J Med Radiat Sci* 2017;**48**(3):233–53.
26. Soares DP, Law M. Magnetic resonance spectroscopy of the brain: review of metabolites and clinical applications. *Clin Radiol* 2009;**64**(1):12–21.
27. Roebuck JR, Cecil KM, Schnall MD, *et al*. Human breast lesions: characterization with proton MR spectroscopy. *Radiology* 1998 Oct;**209**(1):269–75.
28. Gribbestad IS, Singstad TE, Nilsen G, *et al*. *In vivo* ^{1}H MRS of normal breast and breast tumours using a dedicated double breast coil. *J Magn Reson Imaging* 1998 Nov;**8**(6):1191–7.
29. Yeung DK, Yang WT, Tse GM. Breast cancer: *in vivo* proton MR spectroscopy in the characterization of histopathologic subtypes and preliminary observations in axillary node metastases. *Radiology* 2002;**225**(1):190–7.
30. Yeung DK, Cheung HS, Tse GM. Human breast lesions: characterization with contrast-enhanced in vivo proton MR spectroscopy—initial results. *Radiology* 2001;**220**(1):40–6.
31. Montemezzi S, Cavedon C, Camera L, *et al*. ^{1}H-MR spectroscopy of suspicious breast mass lesions at 3T: a clinical experience. *Radiol Med* 2017;**122**(3):161–70.
32. Langhammer R, Cheng LL, Nowak J, *et al*. Metabolomic imaging for human prostate cancer detection using MR spectroscopy at 7-T. *Rofo* 2014;**186**:53.
33. Abd-Alazeez M, Ahmed HU, Arya M, *et al*. The accuracy of multiparametric MRI in men with negative biopsy and elevated PSA level—can it rule out clinically significant prostate cancer? *Urol Oncol* 2014 Jan;**32**(1). 45.e17-22.
34. Bezabeh T, Somorjai R, Dolenko B, *et al*. Detecting colorectal cancer by 1H magnetic resonance spectroscopy of fecal extracts. *NMR Biomed* 2009;**22**(6):593–600.
35. Iorio E, Mezzanzanica D, Alberti P, *et al*. Alterations of choline phospholipid metabolism in ovarian tumour progression. *Can Res* 2005;**65**(20):9369–76.
36. Takeuchi M, Matsuzaki K, Harada M. Differentiation of benign and malignant uterine corpus tumours by using proton MR spectroscopy at 3T: preliminary study. *Eur Radiol* 2011;**21**(4):850–6.
37. Takeuchi M, Matsuzaki K, Harada M. Preliminary observations and clinical value of lipid peak in high-grade uterine sarcomas using *in vivo* proton MR spectroscopy. *Eur Radiol* 2013 Sep 1;**23**(9):2358–63.
38. Huang W, Fisher PR, Dulaimy K, *et al*. Detection of breast malignancy: diagnostic MR protocol for improved specificity. *Radiology* 2004 Aug;**232**(2):585–91.
39. Zhang J, Cai S, Li C, *et al*. Can magnetic resonance spectroscopy differentiate endometrial cancer? *Eur Radiol* 2014 Oct 1;**24**(10):2552–60.
40. Johnson W, Taylor MB, Carrington BM, *et al*. The value of hyoscine butylbromide in pelvic MRI. *Clin Radiol* 2007 Nov 1;**62**(11):1087–93.
41. Ananthakrishnan G, Macnaught G, Hinksman L, *et al*. Diffusion-weighted imaging in uterine artery embolisation: do findings correlate with contrast enhancement and volume reduction? *Br J Radiol* 2012 Nov;**85**(1019):e1046–50.
42. Koh DM, Collins DJ. Diffusion-weighted MRI in the body: applications and challenges in oncology. *AJR Am J Roentgenol* 2007 Jun;**188**(6):1622–35.
43. Koyama T, Togashi K. Functional MRI of the female pelvis. *J Mag Reson Imaging* 2007 Jun;**25**(6):1101–12.